HELLENIC REPUBLIC

National and Kapodistrian University of Athens

Department of Biology

Athens International Master's Programme in Neurosciences

Biomedical Sciences Research Center "Alexander Fleming"

RESEARCH THESIS PROJECT

Lhx6 controls cIN development on a stage and IN-subtype specific manner

Vasiliki Antonakou 111714

2019

HELLENIC REPUBLIC

National and Kapodistrian University of Athens

Department of Biology

Athens International Master's Programme in Neurosciences

Biomedical Sciences Research Center "Alexander Fleming"

RESEARCH THESIS PROJECT

Lhx6 controls cIN development on a stage and IN-subtype specific manner

Three Member Evaluation Committee	Title
Antonis Stamatakis, Supervisor	Associate Professor of Biology-Biology of Behaviour, Faculty of Nursing
Spiros Efthimiopoulos	Professor of Animal & Human Physiology-Neurobiology
Panos Politis	Principal Investigator, Biomedical Research Foundation of the Academy of Athens

2019

CONTENTS

Lhx6 controls cIN development on a stage and IN-subtype specific manner

Vasiliki Antonakou[1] 111714

1. *Development and Function of Cortical Interneurons Lab, B.S.R.C. "Alexander Fleming", 34 Fleming str., Vari 166 72, Greece*

SUMMARY

Inhibitory interneurons comprise one of the two main classes of cortical neurons that are essential for the assembly and function of cortical neural circuits. Deficits of the GABAergic system have been implicated in the etiology of several neurodevelopmental disorders. Recently, we have generated transgenic mice, in which the transcription factor Lhx6, that is essential for the development of Medial Ganglionic Eminence (MGE)-derived, Parvalbumin (PV) and Somatostatin (SST) expressing cortical interneurons (cINs), can be deleted in a stage and cell-type specific manner. Mice in which Lhx6 has been deleted in MGE-derived cINs during embryogenesis, show several defects in their differentiation and maturation. On the other hand, when Lhx6 is deleted during early postnatal stages in PV-expressing cINs, we observe a less dramatic phenotype. To understand the mechanism of Lhx6 function in each developmental process, we have performed genome-wide profiling (RNA-seq) for both mutant lines. Our results will elucidate the impact of Lhx6 function in gene regulatory networks controlling distinct stage and cell-type specific processes during cortical interneuron development.

HIGHLIGHTS

- Mice in which Lhx6 has been deleted during embryogenesis fail to differentiate and acquire their mature functional properties.
- Mice in which Lhx6 has been deleted from PV-expressing interneurons at early postnatal stages, show a progressive loss of their mature attributes.

KEYWORDS

MGE-derived cortical interneurons, parvalbumin, Lhx6, maturation, survival

INTRODUCTION

The mammalian cortex comprises two neuronal populations: the excitatory pyramidal neurons (PN), and the inhibitory, γ-aminobutyric acid (GABA) producing interneurons (cINs). Cortical INs are crucial in regulating and orchestrating the

function of PNs. Indeed, the interplay between these two neuronal populations is fundamental for the balance between excitation and inhibition, that is essential for normal brain function. As a result, even minor defects in cortical interneurons have been implicated in the etiology of several neurodevelopmental disorders such as autism, epilepsy and schizophrenia [1].

The cerebral cortex is populated with more than 20 different types of GABAergic neurons, all derived from progenitors located in the subpallium, the ventral part of the embryonic telencephalon [2]. Regarding rodents and primates, including humans, the subpallium can be subdivided into several proliferating regions. Among these regions the Medial Ganglionic Eminence (MGE), the caudal GE (CGE) and the preoptic area (POA) are considered to be the major sources of cINs (Fishell & Rudy, 2011). Although, the place of origin defines certain aspects of IN identity, it is only when they reach their final position within the cortex and make contacts with the local circuitry that cINs acquire their mature properties and become morphologically and functionally distinguishable from each other. This protracted period of cIN development, led to the hypothesis that their identity is specified progressively and not exclusively at the progenitor level [4,5].

Approximately 60% of all cINs arise in the MGE, and give rise to PV- and SST-expressing INs (Fishell & Rudy, 2011). The most abundant cIN population is the PV^+ INs, which can be further subdivided into the basket cells, which form synapses at the dendrites and somata of PNs, and the chandelier cells, which primarily target the axonal initial segment. PV^+ INs are of prime interest, since their function is increasingly linked to the production of synchronized neural network oscillations, which by facilitating the processing and flow of information within the brain, are essential for normal cognitive function [2].

We and others have previously demonstrated that the LIM homeodomain (HD) transcription factor LHX6 plays a pivotal role in the generation of both MGE-derived cortical interneurons. More specifically, Lhx6 KO mice have multiple defects in several steps of cIN development, such as migration, laminar acquisition, and marker expression, as well as, the formation of functional inhibitory circuits [6–8]. In addition, it has been recently suggested that Lhx6 might have an important role in the survival of MGE-derived cortical interneurons, although the mechanism remains to be elucidated [9]. Although, all published evidence demonstrate that Lhx6 controls

the development of all MGE-derived interneurons, there is no doubt that the unfolding of Lhx6-dependent differentiation and maturation programs follows subtype-specific spatiotemporal patterns. This is underscored by the differential spatiotemporal expression profile of subtype markers, such as PV and SST. Both Pv mRNA and protein are expressed only at relatively late stages of interneuron development in the postnatal cortex [10] In contrast, Sst mRNA is expressed during embryogenesis by tangentially migrating immature interneurons, although the SST peptide is detected exclusively in postnatal animals [8,10].

In order to begin unraveling the mechanism of Lhx6 function in each developmental process in a time and subtype specific manner, we have generated transgenic mice in which: a) Lhx6 is deleted at early embryonic stages in both SST- and PV interneuron progenitors, to study its role in common pathways determine early differentiation steps during the critical developmental window of the first two postnatal weeks, b) Lhx6 is deleted in PV-expressing only cINs, from postnatal day 10 (P10) and onwards, in order to address the impact of Lhx6 function on the maturation and the maintenance of the mature identity of PV expressing cINs, specifically. Our results show that Lhx6 has distinct stage and cell-type specific functions during cIN development.

METHODS

1. Animals

1.1 Mouse lines

Lhx6flox mice used in this study were generated via homologous recombination, taking advantage of the CRELoxP system using a targeting construct in which loxP sites were placed in non-coding regions just 5' to coding exon 1b, and 3' to coding exon 3 as previously described [9]. Tg(Nkx2-1-cre)1Wdr (MGI:3761164, [11], shorted here as Nkx2.1-Cre, transgenic mice were kindly provided by N. Kessaris, (University College London UK) and B6;129P2-*Pvalb*$^{tm1(cre)Arbr}$/J shorted here as PV-Cre mice [12] were imported from the Jackson Laboratory (stock number: 008069) donated by Silvia Arber (Friedrich Miescher Institute, Switzerland). In order to trace Cre-expression two different Cre-dependent transcription reporters, Rosa26eYFP (GFP variant) [13] or Rosa26tdTomato (RFP variant, B6;129S6-Gt(ROSA)26Sor$^{tm9(CAG-}$

tdTomato)Hze/J, The Jackson Laboratory ®) were inserted by crossing with Lhx6flox line with the aforementioned mouse lines.

1.2 Animal husbandry

Mice were housed, bred and handled according to the guidelines of the Presidential Decree No 160/1991 (Governmental Gazette No A' 64) applicable in Greece. Mattings were set up in the afternoon and the presence of a vaginal plug (VP) was checked the next morning, defining the embryonic day 0.5 (E0.5). For postnatal animals the day of birth was considered as postnatal day 0 (P0).

2. Molecular biology techniques

2.1 DNA extraction

DNA was obtained from mice by toe amputation or by tail clip, and incubated in 500 µl Proteinase K lysis buffer (100 mM Tris-HCl pH 8.5, 5 mM EDTA pH 8.0, 0.2% SDS, 200 mM NaCl, Proteinase K (0.1 mg/ml; Roche, 03 115 879 001) at 55°C overnight. DNA was precipitated by adding 500 µl of isopropanol, mixing and centrifuging at 13500 rpm for 15 minutes at room temperature. The supernatant was discarded and the pellets were left to air-dry and finally re-suspended in 100 µl of H_2O for injection.

2.2 RNA extraction

Total RNA was extracted from FACS purified cells using an RNeasy Micro Kit (QIAGEN, Cat. No. 74004) following the manufacturer's instructions. Briefly, sorted cells were lysed with Extradiol, then mixed with chloroform centrifuged at 12000 x g for 15 minutes at 4°C. The colorless phase containing the RNA was washed with ethanol and applied to a PureLink Micro Kit Column. A series of washing steps was used in order to remove proteins, DNA, and other contaminants, while the bound RNA was eluted in 20 µl of RNase-free dH_2O and stored at -80°C.

2.3 Plasmid DNA amplification

For plasmid DNA amplification, plasmid DNA (10 pg - 100 ng) was transformed into One Shot® TOP10 chemically competent E. coli cells (Invitrogen, C4040). First, a 50 µl aliquot of the competent cells was thawed on ice, combined with the plasmid and incubated on ice for 30 minutes. Then, the cells were heat-shocked at 42°C for 30 seconds, in order to uptake the DNA, and subsequently returned on ice for 30 seconds. Working under aseptic conditions, 250 µl of LB medium were added to the cells, which were then allowed to recover in a 37°C

incubator, shaking at 225 rpm for 1 hour. 100 µl of the cell suspension were then plated onto a pre-warmed at 37°C LB agar plate containing 100 µg/ml of ampicillin. The plates were incubated upside down at 37°C overnight and the next day they were examined for the presence of antibiotic-resistant colonies.

A single colony was then used to inoculate 5 ml of LB medium containing 100 µg/ml ampicillin and incubated at 37°C, shaking at 225 rpm overnight. The mini-culture was then diluted 1/500 in LB with 100 µg/ml ampicillin and left to grow while shaking at 37°C, in order to produce a bacterial maxi-culture. After 12-16 hours, bacterial cells were collected by centrifugation at 6000 x g for 15 minutes at 4°C and processed for plasmid DNA extraction.

2.4 Plasmid DNA extraction

QIAfilter Plasmid Maxi Kit (QIAGEN, Cat. No. 12262) was used for the isolation and purification of plasmid DNA according to the manufacturer's instructions. Briefly, after alkaline lysis of bacterial pellets, the plasmid DNA was allowed to bind to a resin column under low- salt conditions. Using a high-salt buffer, DNA was eluted and afterwards precipitated using isopropanol, while proteins, RNA and other contaminants were washed off. DNA was finally eluted in 500 µl ddH_2O and stored at -20°C.

2.5 Restriction enzyme digestion

Diagnostic digestions of plasmid DNA were performed using 1µg of DNA, 2 µl of enzyme-specific 10x digestion buffer (Roche), 0.5 µl of the suitable restriction enzyme (10 U/µl) (Roche) and ddH_2O up to a final volume of 20 µl. The reactions were incubated for 1 hour at 37°C and loaded on a 1% agarose gel for electrophoresis.

2.6 Riboprobe synthesis

Digoxigenin (DIG)-labeled riboprobes used in RNA *in situ* hybridisation were generated by *in vitro* transcription by combining 1.5 µg of linearised plasmid, 4 µl of 5x transcription buffer (Promega, P118B), 2 µl of 100mM DTT (Promega, P117B), 2 µl of 10x DIG labeling mix (Roche, 11277073910), 0.5 µl of Rnasin RNase inhibitor (Promega, N211B), 1.5 µl of the required RNA polymerase (10 units/µl, T7 Promega, P207B; T3 Promega, P208C) and RNase-free dH_2O up to 20 µl. The reaction was incubated at 37°C for a maximum of 2 hours. In 1 hour of incubation, 1 µl of the reaction was run on a 1% agarose gel to check for the presence of an RNA transcript.

In the presence of RNA, 2 µl of RQ1 DNase I (Promega, M198A) were added to the reaction and incubated at 37°C for 15 minutes. After elimination of plasmid DNA, the probes were precipitated by adding 100 µl TE, 10 µl 4M lithium chloride (LiCl) and 300 µl of 100% EtOH and incubating at -20°C for at least 30 minutes. The reaction was then centrifuged at 13500 rpm for 10 minutes. The RNA pellet was washed with 70% EtOH, air-dried, dissolved in 50 µl TE and stored at -20°C. A full list of the antisense riboprobes used in this thesis, along with the restriction enzymes and RNA polymerases used for their generation is presented in Table 1.

Table 1. Antisense riboprobes, restriction enzymes and RNA polymerases used for their generation

Riboprobes	Restriction Enzymes	RNA polymerase
Arc	BamHI	T7
Egr1	EcoRI	T7
c-fos	EcoRI	T7

2.7 Polymerase chain reaction (PCR)

PCR was performed using 10x buffer (Invitrogen, P/N y02028), 50 mM MgCl2 solution (Invitrogen, P/N y02016), a mix of 10 mM dNTPs (set of dATP, dCTP, dGTP, dTTP, each at 100 mM, Invitrogen, 10297-018), appropriate primers, Taq DNA polymerase (Invitrogen, 18038-026), and ddH_2O. Primer stocks (Sigma-Genosys) were ordered in lyophilized form and re-suspended in ddH_2O to a final concentration of 100 µM.

Reactions for the Cre, iCre and R26ReYFP PCRs were performed in a final volume of 25 µl, by adding 1 µl of extracted genomic DNA in a mixture of 2.5 µl 10x buffer, 0.75 µl MgCl2, 0.5 µl dNTPs, 0.5 µl forward primer, 0.5 µl reverse primer, 0.2 µl Taq polymerase and 19.05 µl ddH2O. For the Rosa26Tdti14 PCR, reactions were conducted at a final volume of 25 µl, mixing 2 µl of extracted genomic DNA, 19.4 µl MegaBlueMix and 0.9 µl of each primer (4 primers in total). For the Lhx6 PCR, reactions were set up at a final volume of 25 µl using 1 µl of extracted genomic DNA, 2.5 µl 10x buffer, 0.75 µl MgCl2, 0.5 µl dNTPs, 0.5 µl of each primer, 0.25 µl Taq and 19 µl ddH2O.

Details for PCR conditions, primer sequences and expected band sizes for each PCR can be found in Table 2. The presence or absence of PCR products and their size was determined by agarose gel electrophoresis.

2.8 Agarose gel electrophoresis

DNA electrophoresis was performed in 2% (w/v) agarose gel, which was prepared by dissolving agarose in TAE buffer and heating the solution in a microwave oven until the agarose was fully dissolved. EtBr was added in the solution in order to visualize the DNA, and the mixture was then placed into a mold with the suitable well combs and left to congeal. PCR products were mixed with 10x Orange G loading dye (20% Ficoll, 0.1 M EDTA, 1% SDS, 0.25% Orange G) at a ratio of 9:1, loaded onto the gel and electrophoresed at 100-150 V.

Table 2. PCR conditions and primer sequences used in genotyping

MOUSE LINE	**GENE**	**PCR PRIMER SEQUENCES**	**PROGRAM**			**PCR PRODUCTS (~bp)**
			Temp	**Time**	**Cycles**	
	Cre F	5' ATC CGA AAA GAA AAC GTT GA 3'	94 ºC	3'	1	Mut : 550
PVCRE	Cre R	5' ATC CAG GTT ACG GAT ATA GT 3'	94 ºC	1'		
			53 ºC	1'	35	
			72 ºC	1'		
			72 ºC	5'	1	
			4 ºC	Hold		
	R26_R2	5' GCGAAGAGTTTGTCCTCAACC-3'	95 ºC	2'30''	1	
	R26_R3	5' GGAGCGGGAGAAATGGATATG-3'	95 ºC	30"		WT:384
Rosa26EYFP	R26_F	5' GCTCTGAGTTGTTATCAGTAAGG-3'	55 ºC	30"	35	Mut:142
			72ºC	45"		
			72ºC	10'	1	
			4 ºC	Hold		
Rosa26Tdti14	R26_wt-F	5' AAG GGA GCT GCA GTG GAG TA 3'	95 ºC	5'	1	WT:297
	R26_wt-R	5' CCG AAA ATC TGT GGG AAG TC 3'	95 ºC	30"		
	i14_mut-F	5' CTG TTC CTG TAC GGC ATG G 3'	60 ºC	30"	35	Mut:196
	i14_mut-R	5' GGC ATT AAA GCA GCG TAT CC 3'	72ºC	45"		

			72ºC	7'	1	
			4 ºC	Hold		
			95 ºC	5'	1	
Floxed Lhx6	P1-F	5' GGA GGC CCA AAG TTA GAA CC 3'	94 ºC	30"		
(Lhx6flox)	P2-R	5' CTC GAG TGC TCC GTG TGT C 3'	63 ºC	45"	35	Mut: 350
			72ºC	1'		
			72ºC	10'	1	
			4 ºC	Hold		
			94 ºC	5'	1	
			94 ºC	45"		
Nkx2.1iCRE	NkxCRE-F	5' GTC CAC CAT GGT GCC CAA GAA GAA G 3'	60 ºC	1'	30	Mut:500
	NkxCRE-R	5' GCC TGA ATT CTC AGT CCC CAT CTT CGA GC 3'	72ºC	1'		
			72ºC	10'	1	
			4 ºC	Hold		

3. Tissue manipulation techniques

3.1 Perfusion and adult brain dissection

Adult mice were anaesthetised by intraperitoneal injection of 0.05 ml/10 g of Ketamine/Xylozine (100/6.6) (Drug Stock of ketamine: 100 mg/ml and xylozine: 20 mg/ml) and subsequently transcardially perfused with 0.9% (w/v) NaCl in ddH_2O, followed by 4% PFA in PBS. Brains were then dissected out of the scull and post-fixed in 4% PFA at 4^{o}C overnight.

3.2 Tissue freezing and cryosectioning

Fixed postnatal brains were washed in PBS (3x10 min, @RT), and cryoprotected in 15% sucrose (VWR, 27480.294) in PBS overnight at 4^{o}C. The next day they were changed to 30% sucrose in PBS and left overnight at 4^{o}C. Then, they were embedded in a mix of 7.5% gelatin (Sigma-Aldrich, G2500) /15% sucrose in PBS, at 4^{o}C until set, and frozen in Isopentane (Sigma-Aldrich, 154911) cooled at -60^{o}C.

Using a cryostat (Leica CM1950) serial cryosections at 12 µm were collected on Superfrost Plus glass slides (Thermo Scientific, J1800AMNZ) and stored at -20^{o}C, or used directly for immunohistochemistry or in situ hybridisation.

3.3 Vibratome sectioning

Fixed brains from postnatal animal were washed in PBS (3x10 min). A vibratome (Leica, VT1200S) was required for floating sections of 100 µm, which were transferred to 24-well plates (NUNC, 142485) containing PBS and stored at 4^{o}C. In case of long-term use, 0.05% NaN3 (Sigma-Aldrich, 13412) was added to the PBS to preserve tissue quality.

3.4 Fluorescence-activated cell sorting (FACS)

FACS procedure was performed according to the protocol published in Biotechniques (Saxena et al., 2012). Briefly, mice were euthanatized by cervical dislocation and their whole brains were dissected. The cortex was removed and placed in a Petri dish containing 5 ml equilibrated mixed EBSS#1 solution [EBSS, 100 mM AP-V (DL-AP5, Cat # 0105 Tocris Bioscience), 100 mM Kynurenic acid (KA) (K-3375, Sigma-Aldrich), 50% (w/v) Trehalose (Sigma-Aldrich Catalog # 90208)] and cut in small pieces. The shattered tissue was transferred in 50 ml tube and the remained EBSS was discard. Then, in the tube was added 2.5 ml Papain DNase I solution added in Papain solution (100 units of papain in 1 mM L-cysteine and 0.5 mM EDTA added in 5 ml of EBSS#1 and incubated for 10 min in 37^{o}C) and incubated for 1 hour at 37^{o}C. After incubation, 2.5 ml of EBSS#2 (EBSS, 100 mM AP-V, 100 mM KA, Albumin-ovomucoid inhibitor, DNase I, 50% (w/v) trehalose) was added and gently mixed by avoiding air bubbles. The suspension was centrifuged at 1200 rpm for 10 min and the pellet was re-suspended with 150 µl of EBSS#2. Mechanically dissociation was performed by pipetting up and down gently 20-30 times. Then, 100 µl EBSS#2 was added and mixed 15 times with pipette in order to achieve a homogenous cell suspension. Following addition of 5 ml of medium without serum [DMEM/F-12 without phenol red (Gibco, 11039–021, Invitrogen), 50% (w/v) trehalose, 100 mM AP-V, 100 mM KA] and centrifugation at 15000 rpm for 10 min, the pellet was re-suspended with 200 µl EBSS#2 and by pipetting gently another 5 ml of medium without serum was added and the mixture was centrifuged at 15000 rpm for 10 min. Then, the final pellet was re-suspended with 1 ml of medium with serum [DMEM/F-12 without phenol red, Fetal Bovine Serum (FBS) (cat # 12103C-100ML, Nichirei co.), horse serum (26050–070, 100 mL Gibco) , 50% (w/v) trehalose, 100 mM AP-V, 100 mM KA].

The cell suspension was transferred to a flow cytometry polystyrene tube provided with a cell strainer cap (BD, 352235), through which it was filtered to ensure single-cell suspension. Tubes were kept on ice and samples were transferred into a cell sorter (FACS AriaII, Becton-Dickinson). Approximately 40 MGEs, yielded 10,000-30,000 RFP^+ or GFP^+ cells, which were collected into individual RNase-free tubes containing TRIZOL LS (10296010 100ML Invitrogen), and immediately processed for RNA extraction.

4. Histochemistry techniques

4.1 Immunohistochemistry (IHC)

4.1.1 IHC on cryostat sections

Cryostat sections from postnatal animals were rinsed in PBT (0.1% Triton X-100 in 1X PBS) (3x10 min, RT) and incubated in blocking solution [10% Donkey Serum (DK) (D9663, LifeScienceChemilab) in PBT] for at least 1 hour at room temperature. Primary antibodies were added in blocking solution (1% DK in PBT) and applied on the slides at 4°C overnight. The next day, sections were washed in PBT (3x5 min, RT), and incubated with secondary antibodies diluted in blocking solution (1% DK in PBT) at room temperature for 2 hours. After washing in PBT (3x5 min, RT), slides were mounted with Vectashield Fluorescence Anti-fade Mounting Medium (Vector Labs H-1200) which contained DAPI to stain the cell nuclei.

4.1.2 IHC on vibratome sections

Vibratome floating sections were permeabilised in 0.5% Triton X-100 in PBS (30 min, RT, shaking) and incubated in blocking solution (10% DK in 0.1% PBT) for 1 hour while shaking. Primary antibodies were diluted in antibody solution (1% DK in 0.1% PBT) and incubated in cold room (4°C, shaking, overnight). The next day, sections were washed in 0.1% PBT and incubated with secondary antibodies diluted in antibody solution (1 h, RT, shaking). After washing in 0.1% PBT (3x10 min, RT, shaking), sections were transferred on to slides by using a paintbrush, left to dry and mounted with Vectashield mounting medium with DAPI.

The list of primary and secondary antibodies used in this thesis is presented in Table 3.

Table 3. List of primary and secondary antibodies

Primary antibodies	**Host**	**Dilution**	**Supplier**
Lhx6	Rabbit	1/500	Pachnis Lab [14]
GFP	Rabbit Rat	1/1000 1/500	Molecular Probes (Invitrogen) (Cat. No. A11122) Nascalai Tesque Inc. (Cat. No. 04404-84)
Sox6	Rabbit	1/1000	Abcam (Cat. No. AB30455)
Satb1	Goat	1/500	Santa-cruz (Cat. No. sc5990)
SST	Rat	1/500	Millipore (Cat. No. MAB354)
NPY	Rabbit	1/1000	Peninsula Laboratories (Cat. No. T-4070)
PV	Rabbit	1/1000	Swant PV25
cfos	Rabbit	1/4000	Promega ABE457
VIP	Rabbit	1/1000	Immunostar 20077
Mafb	Rabbit	1/1000	BETHYL LABS IHC-00351
Wisteria Floribunda Lectin (WFA)	Biotinylated	1/500	Vector Laboratories B-1355
Secondary Antibodies	**Host**	**Dilution**	**Supplier**
Anti-Rabbit	Donkey	1/1000	Alexa Fluor 488 (Molecular Probes Cat. No. A-21206) Alexa Fluor 568 (Molecular Probes Cat. No. A-10042)
Anti-Rat	Donkey	1/1000	Alexa Fluor 488 (Molecular Probes Cat. No. A-21208)
Anti-Goat	Donkey	1/500	Alexa Fluor 647 (Molecular Probes Cat. No. A-21447)

4.2 RNA *in situ* hybridisation

Non-radioactive *in situ* hybridisation was performed on 12 µm thick cryosections of one, two, three and six months old mice. Slides were fixed in 4% PFA

in PBS (10 min, RT) and washed in PBS with 0.1% Tween 20 (3x10 min, RT). Slides were then incubated in acetylation solution [0.1 M Triethanolamine (Fluka 90279), 0.65% of 37% HCl, and 0.375% acetic anhydride in ddH2O] for 10 minutes at room temperature and washed in PBT (3x5 min, RT). Hybridisation solution [50% v/v deionised formamide (SIGMA, F9037), 5x SSC, 5x Denhardt's (Invitrogen, 750018), 250 µg/ml yeast tRNA (SIGMA, R6750) and 500 µg/ml herring sperm DNA (Promega, D1816)] was then applied on the sections and incubated for 1 hour at room temperature. DIG-labelled riboprobe of choice was diluted in hybridisation buffer (1:100), heated at 80^{o}C for 5 minutes and then transferred on ice. 80 µl of the dilution was applied on each slide, coverslipped and incubated in a humidified chamber placed in an oven set at 72^{o}C overnight, along with 5x and 0.2x SSC solution.

The following day, the slides were submerged in 5x SSC solution in order to remove coverslips, washed in 0.2x SSC (1 hour @72^{o}C, then 5 min @RT) and finally equilibrated in buffer B1 (100 mM Tris pH 7.5, 150 mM NaCl) for 5 minutes at room temperature. Slides were then blocked in buffer B1 + 10% heat inactivated sheep serum (1 hour, RT) and incubated with alkaline phosphatase (ALP) conjugated sheep anti-DIG antibody (Roche, 11 093 274 910) which was diluted 1:5000 in buffer B2 (B1 + 1% heat inactivated sheep serum), on horizontally placed slides in a humidified chamber at 4^{o}C overnight.

The next day, the sections were washed with buffer B1 (3x5 min, RT) and then incubated in buffer B3 (100 mM Tris pH 9.5, 100 mM NaCl, 50 mM MgCl2) for 5 minutes at room tempearture. After this, slides were incubated in B4 [4.5 µl/ml of 75 mg/ml Nitrotetrazolium Blue chloride (NBT; Sigma-Aldrich, N6639, diluted in 70% dimethylformamide) and 3.5 µl/ml of 50 mg/ml 5-Bromo-4-chloro-3-indolyl phosphate disodium (BCIP; Sigma-Aldrich, B6149, diluted in ddH2O) in buffer B3] in a humidified chamber kept in the dark at room temperature, and checked every couple hours for staining and stopped the reaction, by washing the slides with PBS. Finally, the slides were mounted with Aquatex® aqueous mounting agent (Merck Millipore, 108562).

5. Image processing and analysis

Bright field images of *in situ* hybridised sections were acquired with a digital colour camera attached to a microscope (Nikon Eclipse E800). All fluorescent images

were captured with a confocal laser-scanning microscope (Leica TCS SP8x) using standard excitation and emission filters to visualise DAPI, Alexa Fluor 488, Alexa Fluor 568 and Alexa Fluor 647. Figures of both bright field and fluorescence images were composed using the Adobe Photoshop CS4 (Adobe Systems) software.

6. Quantification and statistical analysis

Cell countings and colocalization of Lhx6 with GFP and various interneuronal markers over GFP^+ ratios were performed on coronal cortical sections from 3 adult mice per genotype. For confocal images, we counted cells double positive cells expressed as a fraction of total GFP+ population for each brain, focusing mostly on S1BF, Br 0.38 mm. Besides cell counting, we measured the size of somata at all ages, by randomly picking cells in different equally separated grids with an oval shaped region of interest (ROI) drawn just inside the soma region of cells that were judged to be in focus. The area size of the ROIs was measured. All imaging and analysis were done by an experimenter blind to the experimental condition. All data are presented as mean ± standard error of the mean. Statistical significance between data sets was determined using the Student's t-test function (two-tailed distribution, two-sample equal variance) in Excel Microsoft and they were considered significant when $p<0.05$ (*), $p<0.01$ (**) and $p<0.001$ (***). Histograms were generated in Excel.

RESULTS

Transcriptomic analysis of Lhx6-deficient MGE-derived cINs at early postnatal stages.

Recently, generation of a novel conditional *Lhx6* allele *Lhx6^{fl}* [9], and introduction into the *Lhx6$^{fl/fl}$* genetic background of the Cre-dependent fluorescent reporter *Rosa26-tdTomato* (tdT, Ai14, [15], allowed it us to use Cre drivers for cell type-specific *Lhx6* ablation and simultaneous fate-mapping of the mutant lineages. Employing this genetic approach, we have initially used the *Nkx2.1Cre* transgenic driver [11], to specifically delete *Lhx6* from early embryonic stages and track Lhx6-deficient MGE-derived cINs. Analysis of the overall number of tdT-expressing cells in the cortex of P18 *Nkx2.1Cre;Ai14;Lhx6$^{fl/fl}$* mice showed a significant reduction relative to controls, suggesting that in addition to its well-established role in cIN subtype specification, *Lhx6* is also required for the survival of MGE-derived cINs [9]. Nevertheless, the mechanism underlying this novel role of Lhx6 in MGE-derived cIN survival has not been studied. To examine this, we performed RNA sequencing to

compare the global transcriptome of tdT-expressing cells from control *Nkx2.1Cre;Ai14;Lhx6*$^{fl/+}$ and *Nkx2.1Cre;Ai14;Lhx6*$^{fl/fl}$ mutant mice, at postnatal day 7 (P7), a stage at which apoptosis of MGE-derived cINs is at its highest [16]. Differential gene expression analysis identified 589 genes that were significantly downregulated (265) or upregulated (324) in mutant relative to control littermates (Figure 1; selection criteria log2-fold change >1 or <-1 with an adjusted p-value of <0.05). In addition to Lhx6 (which was absent for mutant samples), Sox6, Satb1 and Mafb were among the top down-regulated genes in Lhx6 mutants (Figure 1), as well as Sst and Pv, in agreement with previously reported [9] and our current immunohistochemistry data (Figure S1A-F).

A

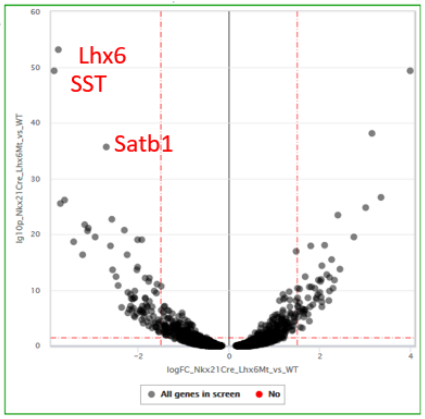

B

Gene	altname	log2FoldChange	p-value
ENSMUSG00000026890	Lhx6	-3,76081929136056	1,29817732565362E-57
ENSMUSG00000004366	Sst	-3,85928516436803	1,13492741728805E-53
ENSMUSG00000023927	Satb1	-2,69756516551062	1,00893295963557E-39
ENSMUSG00000074622	Mafb	-2,30855808025535	2,64531020469754E-24
ENSMUSG00000051910	Sox6	-0,808478309870058	0,00055819231314245 3
ENSMUSG00000005716	Pvalb	-0,849357655933914	0,0209746198065066

Figure 1. Transcriptomic analysis of Lhx6-deficient MGE-derived cINs at early postnatal stages. (A) Scatterplot of differentially expressed genes from RNA-seq of P7 cortices of control and mutant mice. On the right are depicted the upregulated genes and on the left the downregulated. **(B)** Lhx6, SST, Satb1 and Mafb are on the top of the list of downregulated genes, which also includes PV and Sox6, known markers of MGE-derived cINs.

Deletion of Lhx6 at late postnatal stages does not affect the survival of PV-expressing cINs.

To investigate whether Lhx6 has a similar role in the survival of PV-expressing INs when deleted after the critical time window of cIN apoptosis (P6-P10; [16,17], we have crossed the *PvCre* transgenic driver [12], to the *Rosa26-eYFP;Lhx6*^{fl} genetic background [13]. In this experimental set-up, the eYFP fluorescent reporter tracks PV^{+} neurons. It is worth mentioning, that under the specific transgenic driver, eYFP expression is first observed in P10 cortices in a small number of neurons of the PV-lineage, but by P30 all PV-expressing cINs co-express eYFP [12] and data not shown).

We first examined the efficiency of *Lhx6* deletion, in one month old mice. The population of Lhx6^{+} cINs was dramatically decreased in *PVCre;Rosa26eYFP;Lhx6$^{fl/fl}$* mice relative to *PVCre;Rosa26eYFP;Lhx6^{fl+l}* controls (data not shown). Nevertheless, the overall number of eYPF-expressing cells in the cortex of 1, 2, 3 and 6 months old *PVCre;Rosa26eYFP;Lhx6$^{fl/fl}$* mice was similar relative to controls (Figure 2 and FigureS2), suggesting that Lhx6 function is important for PV IN survival only when deleted before the early postnatal critical time window for IN apoptosis.

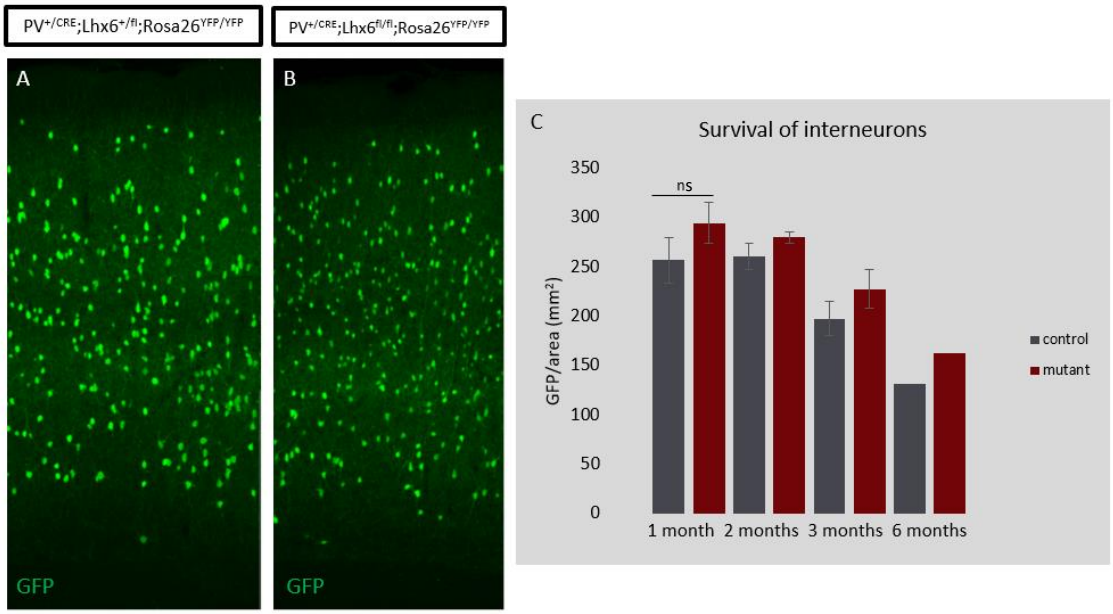

Figure 2. Deletion of Lhx6 at late postnatal stages does not affect the survival of PV-expressing cINs. (A, B) Cryosections from the somatosensory cortex of P30, P60, P90 and P120 control PV$^{+/CRE}$;Lhx6$^{+/fl}$;Rosa26$^{YFP/YFP}$ **(A)** and mutant PV$^{+/CRE}$;Lhx6$^{fl/fl}$;Rosa26$^{YFP/YFP}$ **(B)** littermates were immunostained with polyclonal antibody against GFP. **(C)** Note the overall number of eYPF-expressing cells in the cortex of 1, 2, 3 and 6 months old *PVCre;Rosa26eYFP;Lhx6$^{fl/fl}$* mice was similar relative to controls. Data expressed as mean ± SEM. Student's t-test (two-tailed distribution, two-sample equal variance). 1 month (n=3 animals per genotype), 2 months ($n_{control}$=2 animals, n_{mutant}=3 animals), 3 months ($n_{control}$=1 animal, n_{mutant}=3 animals), 6 months (n=1 animal per genotype).

Aberrant molecular and cellular properties in PV-expressing cINs in the absence of Lhx6 function.

Analysis of both *Lhx6* null and *Nkx2.1Cre;Lhx6^{fl}* mutant mice demonstrated that in the absence of Lhx6 function MGE-derived cINs fail to initiate the molecular cascades that drive their differentiation and maturation [6,7,9]. To investigate whether Lhx6 has an additional role in the maintenance of the mature properties of PV-

expressing cINs, we examined a number of markers associated with cIN differentiation, whose expression is maintained in PV^{+} cINs, throughout adulthood. We observed no differences in the percentage of eYFP cINs co-labelled with antibodies against Pv and Sox6 in one month old *PVCre;Rosa26eYFP;Lhx6$^{fl/fl}$* mice relative to *PVCre;Rosa26eYFP;Lhx6$^{fl/+}$* controls (Figure S3). Interestingly, when we extended our analysis in 2 and 6 months old mice, we observed a clear trend for a smaller percentage of eYFP^{+} cells co-expressing PV, Sox6 or Satb1 (Figure 3). These results suggest that PV^{+} cINs in PVCre;Lhx6^{fl} mutant mice become gradually malfunctioned.

We have previously demonstrated that certain morphological characteristics of cINs correlate with their functional status. For example, cINs that fail to mature and integrate into cortical networks, display a smaller soma size [9]. Additionally, mature PV-expressing cINs are characterized by the presence of perineuronal nets, which are specialized extracellular matrix structures responsible for synaptic stabilization [18–20]. Therefore, we assessed the soma size of eYFP^{+} cells, as well as, the percentage of eYFP^{+} cells co-expressing WFA (Wisteria floribunda agglutinin, a marker for perineuronal nets), in *PVCre;Rosa26eYFP;Lhx6$^{fl/fl}$* and *PVCre;Rosa26eYFP;Lhx6$^{fl/+}$* mice, and we observed no dramatic differences (Figure 4).

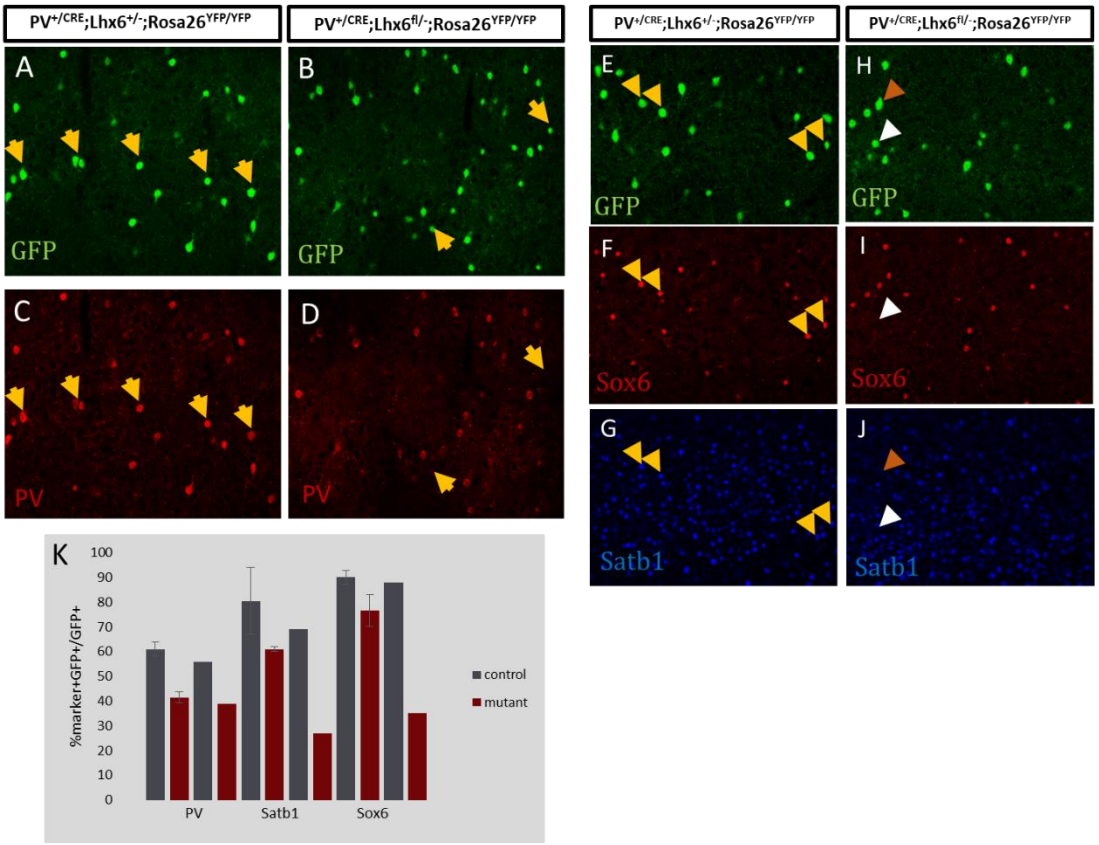

Figure 3. Aberrant molecular properties in PV-expressing cINs in the absence of Lhx6 function. (A-D, G-J) Cryosections from the somatosensory cortex of P60 and P120 control $PV^{+/CRE}$;$Lhx6^{+/fl}$;$Rosa26^{YFP/YFP}$ **(A, C, E, F, G)** and mutant $PV^{+/CRE}$;$Lhx6^{fl/fl}$;$Rosa26^{YFP/YFP}$ **(B, D, H, I, J)** littermates were immunostained with polyclonal antibody against GFP **(A, B, E, H)**, PV **(C, D)**, Sox6 **(F, I)** and Satb1 **(G, J)**. **(K)** Note a clear trend for a smaller percentage of $eYFP^{+}$ cells co-expressing PV **(D)**, Satb1 **(J)** or Sox6 **(I)** compared to the controls **(C)**, **(G)** and **(F)** respectively. Data expressed as mean ± SEM. 2 months ($n_{control}$=2 animals, n_{mutant}=3 animals), 6 months (n=1 animal per genotype).

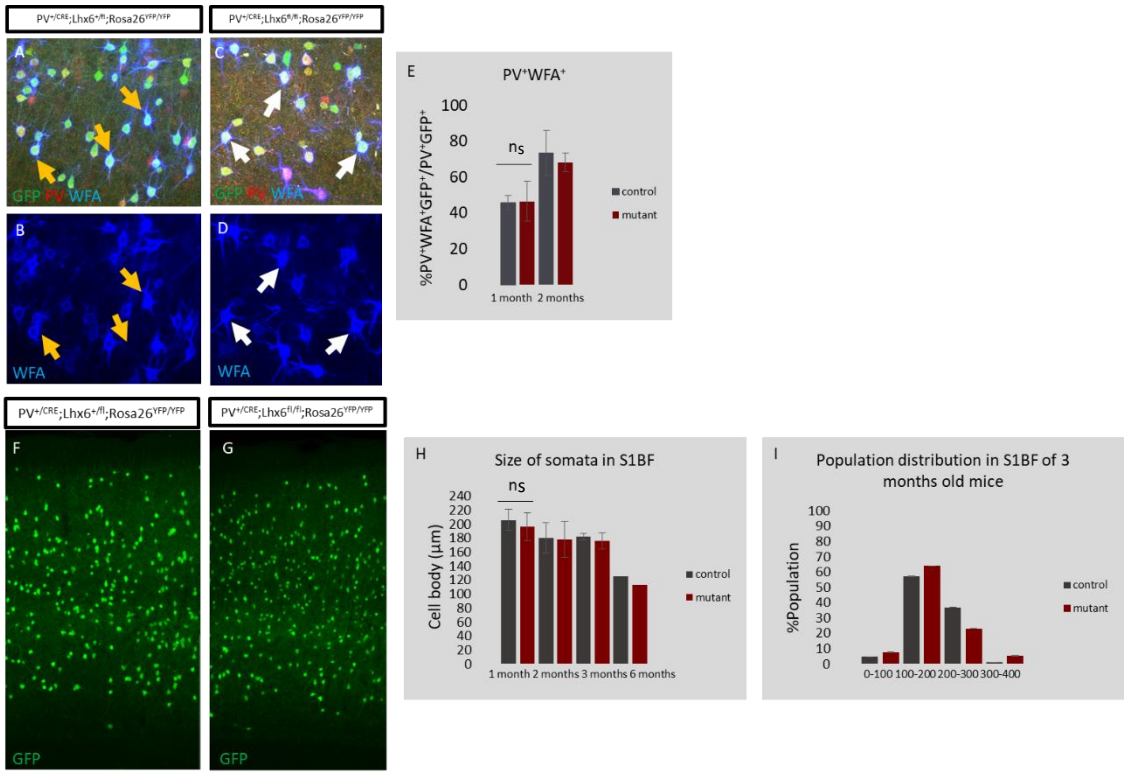

Figure 4. Aberrant cellular properties in PV-expressing cINs in the absence of Lhx6 function. (A-D) Cryosections from the somatosensory cortex of control $PV^{+/CRE}$;$Lhx6^{+/fl}$;$Rosa26^{YFP/YFP}$ **(A, B)** and mutant $PV^{+/CRE}$;$Lhx6^{fl/fl}$;$Rosa26^{YFP/YFP}$ **(C, D)** littermates were immunostained with polyclonal antibody against GFP, PV and WFA **(A,C)** and WFA **(B, D). (E)** Note no differences in the percentage of eYFP cINs co-labelled with antibodies against Pv and WFA in one and two months old *PVCre;Rosa26eYFP;Lhx6*$^{fl/fl}$ mice relative to *PVCre;Rosa26eYFP;Lhx6*$^{fl/+}$ controls. **(F-I)** Measuring the size of cell bodies from one month onwards showed no significant change between control **(F)** and mutant mice **(G)**. **(I)** Population distribution of cell bodies size in S1BF of three months old control and mutant mice. Data expressed as mean ± SEM. Student's t-test (two-tailed distribution, two-sample

equal variance). 1 month (n=3 animals per genotype), 2 months ($n_{control}$=2 animals, n_{mutant}=3 animals), 3 months (n=2 animals per genotype), 6 months (n=1 animal per genotype).

No defects in the number of other cIN lineages in PVCre;Lhx6^{fl} deficient mice.

CGE-derived interneurons are highly connected with both SST^{+} and PV^{+} cINs, and have a fundamental role in controlling their activity [21,22]. Two very well-defined CGE-derived subpopulations are characterized by the expression of the vasoactive intestinal peptide (VIP) [23] and the neuropeptide Y (NPY) (Fishell & Rudy, 2011). Therefore, we performed NPY and VIP immunofluorescence in our mutants to examine for possible defects in the numbers of these populations. We observed no significant reduction in the number of NPY^{+} or VIP^{+} interneurons in *PVCre;Rosa26eYFP;Lhx6$^{fl/fl}$* mutants compare to *PVCre;Rosa26eYFP;Lhx6$^{fl/+}$* control littermates (Figure 5). Our preliminary data, suggest that loss of Lhx6 function in PV-expressing cINs postnatally, does not drive non-cell autonomous defects in other cIN populations, at least in terms of their survival.

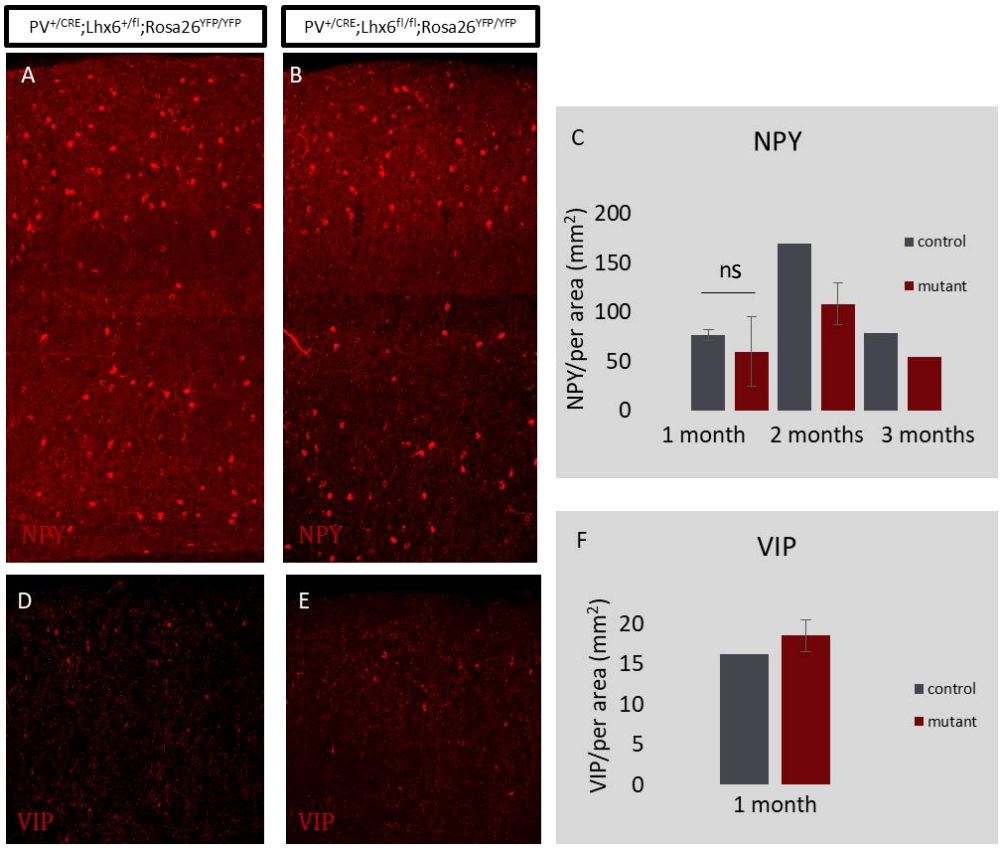

Figure 5. No defects in the number of other cIN lineages in PVCre;Lhx6^{fl} deficient mice. (A-D) Cryosections from the somatosensory cortex of control PV$^{+/CRE}$;Lhx6$^{+/fl}$;Rosa26$^{YFP/YFP}$ **(A, D)** and mutant PV$^{+/CRE}$;Lhx6$^{fl/fl}$;Rosa26$^{YFP/YFP}$ **(B, E)** littermates were immunostained with

polyclonal antibody against NPY (**A, B**) and VIP (**D, E**). (**C, F**) Note no differences in the number of NPY^{+} cells (**C**) and the number of VIP^{+} cells (**F**) in one, two, three months old *PVCre;Rosa26eYFP;Lhx6*$^{fl/fl}$ mice relative to *PVCre;Rosa26eYFP;Lhx6*$^{fl/+}$ controls. Data expressed as mean ± SEM. Student's t-test (two-tailed distribution, two-sample equal variance). 1 month (n=3 animals per genotype), 2 months ($n_{control}$=2 animals, n_{mutant}=3 animals), 3 months (n=2 animals per genotype).

No defects in the expression pattern of IEGs in PVCre;Lhx6^{fl} deficient mice.

Since PV-positive interneuron function is increasingly linked to normal neural network activity, we compared the expression of neuronal activity markers between control and PVCre; *Lhx6*-deficient cortices, at 1, 2, 3 and 6 months old animals. This analysis showed no alteration in the expression pattern of a number of immediate-early genes (IEGs), including the activity-regulated cytoskeleton-associated protein (Arc) [24], the early growth response protein (Egr1) [25] and cfos, between *PVCre;Rosa26eYFP;Lhx6*$^{fl/fl}$ and *PVCre;Rosa26eYFP;Lhx6*$^{fl/+}$ control littermates (Figure 6). Therefore, our results show no gross defects in the overall activity levels in mutant mice.

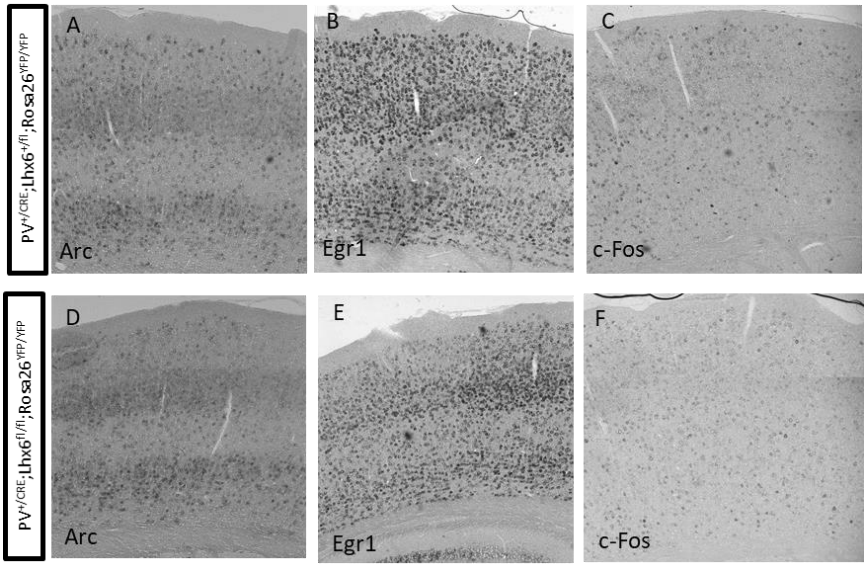

Figure 6. No defects in the expression pattern of IEGs in PVCre;Lhx6^{fl} deficient mice. In situ hybridization of somatosensory cortex sections from control $PV^{+/CRE}$;$Lhx6^{+/-}$;$Rosa26^{YFP/YFP}$ (**A, B, C**) and mutant $PV^{+/CRE}$;$Lhx6^{fl/-}$;$Rosa26^{YFP/YFP}$ (**D, E, F**) two months old mice with either Arc (**A and D**), Egr1 (**B and E**) and c-Fos (**C and F 3 months**) riboprobes shows no alteration of immediately early gene expression in the two littermates. n=1 animal per genotype.

DISCUSSION

In this paper, we used different transgenic lines in which the transcription factor Lhx6 that is essential for the development of cINs [6,7,9], can be deleted in a stage and cell type specific manner, to unravel distinct roles for Lhx6 in different developmental processes and cIN subtypes. For this we have employed: a) the Nkx2.1Cre driver to delete Lhx6 at early embryonic stages in both MGE-derived cIN lineages, and b) the PVCre driver, which results in the deletion of Lhx6, only in the PV-lineage at early postnatal stages (from P10 onwards).

Our preliminary results demonstrate that deletion of Lhx6 after the critical time window of cIN apoptosis (P6-P10; [16], does not results in the cell death of cINs, at least in the PV lineage. This result suggests that Lhx6 function might be redundant for the survival of MGE-derived cINS after P10, but also raises the possibility that the cell death of cINs in the Nkx2.1Cre;Lhx6^{fl} mutant mice might be due to early developmental defects. To distinguish between these two possibilities, we are currently deleting Lhx6 at birth, before the critical period for cIN survival, but when MGE-derived cINs have already reached the cortex. Nevertheless, although, network and cell-intrinsic activity, as well as, Pten-driven signaling cascades have been suggested to be implicated in cIN cell death [9,26,27], the mechanism of cIN apoptosis remains to be elucidated. Therefore, we expect the cIN genome-wide profiling (RNAseq) we had performed in Nkx2.1Cre;Lhx6^{fl} mutant mice, at P7, at the pick of MGE-derived cIN cell death [16], will further enhance our knowledge on this developmental process.

Although, the deletion of Lhx6 in the PV-lineage does not affect the survival of PV^{+} cINs, it has an impact on the expression of several differentiation markers, such as Sox6, Satb1 and PV. Interestingly, a decrease in Lhx6, PV and Satb1 levels is a consistent finding both in human schizophrenics and in animal models of schizophrenia [28,29]. Our analysis for the PVCre;Lhx6^{fl} mutant mice has been mostly performed in the primary somatosensory cortex, since this is one of the best characterized regions for most animal models for cIN development. We are currently expanding our analysis in the hippocampus and the prefrontal cortex, two brain regions that have been thoroughly studied and associated with schizophrenia (Bast, Pezze, & Mcgarrity, 2017). In addition, we expect to gain a lot of valuable information concerning the postnatal role of Lhx6 in the PV^{+} cINs, from the genome-

wide profiling (RNAseq) we had performed in PVCre;Lhx6^{fl} mice. Finally, since the cortices of PVCre;Lhx6^{fl} mutant mice show similar defects, at least at the level of molecular marker analysis, with histological samples obtained from human schizophrenics and animal models of schizophrenia, it would be interesting to further analyze their behavioral phenotype, as well as certain electrophysiological properties of their cortical networks, to examine whether they are associated with a schizophrenia-like phenotype.

ACKNOWLEDGMENTS

This work could have never been conducted without the help and support of my supervisor Antonis Stamatakis and Myrto Denaxa. Dr's Denaxa passion and enthousiasm about science has always been a great inspiration and it was a pleasure going every day in the lab. I would like to give big thanks to her for the opportunity to work on this project and to the lab members (Dimitris, Rania, Yolanta and Giannis) for the great collaboration and beautiful moments inside and outside the lab. Also, I would like to thank Dr's Kostourou Lab members (especially Vasia) for all the guidance needed in microscopes.

REFERENCES

1. Marín O. Interneuron dysfunction in psychiatric disorders. 2012;(January):107-120. doi:10.1038/nrn3155
2. Tremblay R, Lee S, Rudy B. properties to circuits. 2017;91(2):260-292. doi:10.1016/j.neuron.2016.06.033.GABAergic
3. Fishell G, Rudy B. *Mechanisms of Inhibition within the Telencephalon : " Where the Wild Things Are ."* doi:10.1146/annurev-neuro-061010-113717
4. Kepecs A, Fishell G. Interneuron Cell Types : Fit to form and formed to fit. 2015;505(7483):318-326. doi:10.1038/nature12983.Interneuron
5. Wamsley B, Fishell G. Genetic and activity-dependent mechanisms underlying interneuron diversity. *Nat Publ Gr*. 2017. doi:10.1038/nrn.2017.30
6. Liodis P, Denaxa M, Grigoriou M, Akufo-addo C, Yanagawa Y, Pachnis V. Lhx6 Activity Is Required for the Normal Migration and Specification of Cortical Interneuron Subtypes. 2007;27(12):3078-3089. doi:10.1523/JNEUROSCI.3055-06.2007
7. Zhao Y, Flandin P, Long JE, Cuesta M Dela, Westphal H, Rubenstein JLR.

Distinct Molecular Pathways for Development of Telencephalic Interneuron Subtypes Revealed Through Analysis of Lhx6 Mutants. 2008;99(March):79-99. doi:10.1002/cne.21772

8. Neves G, Shah MM, Liodis P, et al. The LIM Homeodomain Protein Lhx6 Regulates Maturation of Interneurons and Network Excitability in the Mammalian Cortex. 2012:1-13. doi:10.1093/cercor/bhs159
9. Denaxa M, Neves G, Rabinowitz A, et al. Modulation of Apoptosis Controls Inhibitory Interneuron Number in the Cortex Article Modulation of Apoptosis Controls Inhibitory Interneuron Number in the Cortex. *CellReports*. 2018;22(7):1710-1721. doi:10.1016/j.celrep.2018.01.064
10. Taniguchi H, He M, Wu P, et al. NeuroResource A Resource of Cre Driver Lines for Genetic Targeting of GABAergic Neurons in Cerebral Cortex. 2011:995-1013. doi:10.1016/j.neuron.2011.07.026
11. Nóbrega-pereira S, Kessaris N, Du T, et al. NIH Public Access. 2009;59(5):733-745. doi:10.1016/j.neuron.2008.07.024.Postmitotic
12. Hippenmeyer S, Vrieseling E, Sigrist M, et al. PLoS BIOLOGY A Developmental Switch in the Response of DRG Neurons to ETS Transcription Factor Signaling. 2005;3(5). doi:10.1371/journal.pbio.0030159
13. Srinivas S, Watanabe T, Lin C, et al. Cre reporter strains produced by targeted insertion of EYFP and ECFP into the ROSA26 locus. 2001.
14. Lavdas AA, Grigoriou M, Pachnis V, Parnavelas JG. The Medial Ganglionic Eminence Gives Rise to a Population of Early Neurons in the Developing Cerebral Cortex. 1999;99(19):7881-7888.
15. Madisen L, Zwingman TA, Sunkin SM, et al. r e so u r c e A robust and high-throughput Cre reporting and characterization system for the whole mouse brain. *Nat Neurosci*. 2009;13(1):133-140. doi:10.1038/nn.2467
16. Southwell DG, Paredes MF, Galvao RP, et al. cortical interneurons. *Nature*. 2012;490(7422):109-113. doi:10.1038/nature11523
17. Lim L, Llorca A. Review Development and Functional Diversification of Cortical Interneurons. 2018. doi:10.1016/j.neuron.2018.10.009
18. Mcrae PA, Porter BE. Neurochemistry International The perineuronal net component of the extracellular matrix in plasticity and epilepsy. *Neurochem Int*. 2012;61(7):963-972. doi:10.1016/j.neuint.2012.08.007

19. Cabungcal J, Steullet P, Morishita H, Kraftsik R, Cuenod M, Hensch TK. Perineuronal nets protect fast-spiking interneurons against oxidative stress. 2013;110(22). doi:10.1073/pnas.1300454110

20. Berretta S, Pantazopoulos H, Markota M, Brown C, Batzianouli ET. Losing the sugar coating : Potential impact of perineuronal net abnormalities on interneurons in schizophrenia. *Schizophr Res*. 2015. doi:10.1016/j.schres.2014.12.040

21. Pfeffer CK, Xue M, He M, Huang ZJ, Scanziani M. Inhibition of inhibition in visual cortex : the logic of connections between molecularly distinct interneurons. *Nat Neurosci*. 2013;(June):1-12. doi:10.1038/nn.3446

22. Pi H. Cortical interneurons that specialize in disinhibitory control. (V). doi:10.1038/nature12676

23. Miyoshi G, Hjerling-leffler J, Karayannis T, et al. Genetic Fate Mapping Reveals That the Caudal Ganglionic Eminence Produces a Large and Diverse Population of Superficial Cortical Interneurons. 2010;30(5):1582-1594. doi:10.1523/JNEUROSCI.4515-09.2010

24. Tzingounis A V, Nicoll RA, Arg A. Arc / Arg3 . 1 : Linking Gene Expression to Synaptic Plasticity and Memory Minireview. 2006;1:403-407. doi:10.1016/j.neuron.2006.10.016

25. French PJ, Connor VO, Jones MW, et al. Sub ® eld-speci ® c immediate early gene expression associated with hippocampal long-term potentiation in vivo. 2001;13:968-976.

26. Wong FK, Bercsenyi K, Sreenivasan V, Portalés A, Fernández-otero M, Marín O. Pyramidal cell regulation of interneuron survival sculpts cortical networks. 2018.

27. Priya R, Paredes MF, Karayannis T, et al. Activity Regulates Cell Death within Cortical Interneurons through a Calcineurin-Dependent Activity Regulates Cell Death within Cortical Interneurons through a Calcineurin-Dependent Mechanism. *CellReports*. 2018;22(7):1695-1709. doi:10.1016/j.celrep.2018.01.007

28. Hashimoto T, Volk DW, Eggan SM, et al. Gene Expression Deficits in a Subclass of GABA Neurons in the Prefrontal Cortex of Subjects with Schizophrenia. 2003;23(15):6315-6326.

29. Lewis DA, Curley AA, Glausier JR, Volk DW. Cortical parvalbumin interneurons and cognitive dysfunction in schizophrenia. *Trends Neurosci*. 2012;35(1):57-67. doi:10.1016/j.tins.2011.10.004

30. Bast T, Pezze M, Mcgarrity S. No Title. doi:10.1111/bph.13850

31. Palop JJ, Mucke L. Network abnormalities and interneuron dysfunction in Alzheimer disease. *Nat Publ Gr*. 2016. doi:10.1038/nrn.2016.141

32. Volk DW, Edelson JR, Lewis DA. Cortical Inhibitory Neuron Disturbances in Schizophrenia : Role of the Ontogenetic Transcription Factor Lhx6. 2014;40(5):1053-1061. doi:10.1093/schbul/sbu068

33. Denaxa M, Kalaitzidou M, Garefalaki A, Achimastou A, Lasrado R, Maes T. Article Maturation-Promoting Activity of SATB1 in MGE-Derived Cortical Interneurons. *CellReports*. 2012;2(5):1351-1362. doi:10.1016/j.celrep.2012.10.003

SUPPLEMENTARY

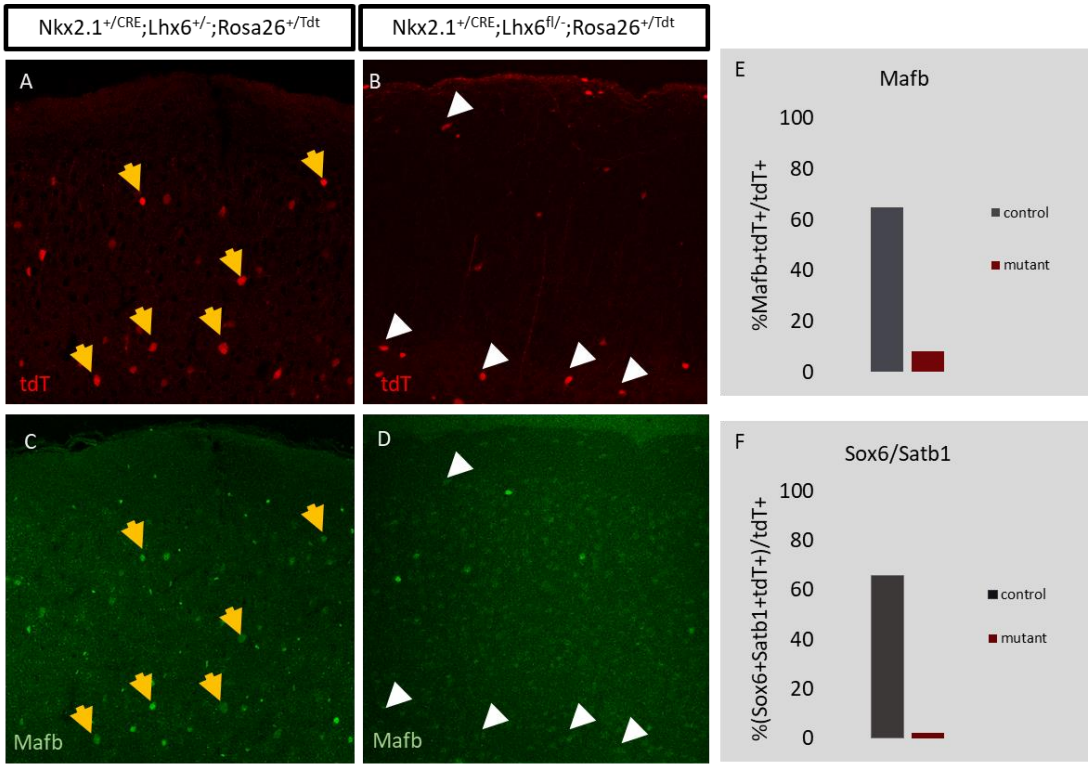

Figure S1. **Differentiation and maturation deficit in Nkx2.1CRE/Lhx6cKO mice. (A, B)** Cryosections from the somatosensory cortex of P18 control Nkx2.1$^{+/CRE}$;Lhx6$^{+/-}$;Rosa26$^{+/Tdt}$ **(A, C)** and mutant Nkx2.1$^{+/CRE}$;Lhx6$^{fl/-}$;Rosa26$^{+/Tdt}$ **(B, D)** littermates were immunostained with polyclonal antibodies against Mafb (**A, B**) or Sox6, Satb1 (data not shown). Note a large fraction of cortical interneurons (tdT^{+}) expresses Mafb in control, but not in mutant sections. **(E, F)** Quantification of the colocalization of MGE markers in control and mutant mice. Note the dramatic reduction of MGE specific cortical interneuron markers Mafb **(E)** and Sox6/Satb1 **(F)** in mutant mice. n=1 animal per genotype.

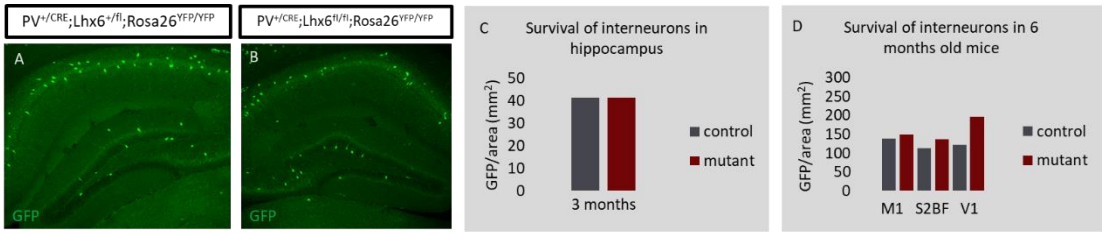

Figure S2. Deletion of Lhx6 at late postnatal stages does not affect the survival of PV-expressing cINs in hippocampus and other brain regions. (A, B) Cryosections from the hippocampus of P90 control PV$^{+/CRE}$;Lhx6$^{+/fl}$;Rosa26$^{YFP/YFP}$ **(A)** and mutant PV$^{+/CRE}$;Lhx6$^{fl/fl}$;Rosa26$^{YFP/YFP}$ **(B)** littermates were immunostained with polyclonal antibody against GFP. **(C, D)** Note the overall number of eYPF-expressing cells in the hippocampus and the primary motor cortex (M1), the secondary barrel field (S2BF) and the primary visual

cortex (V1) of 3 and 6 months old *PVCre;Rosa26eYFP;Lhx6*$^{fl/fl}$ mice, respectively was similar relative to controls. n=1 animal per genotype.

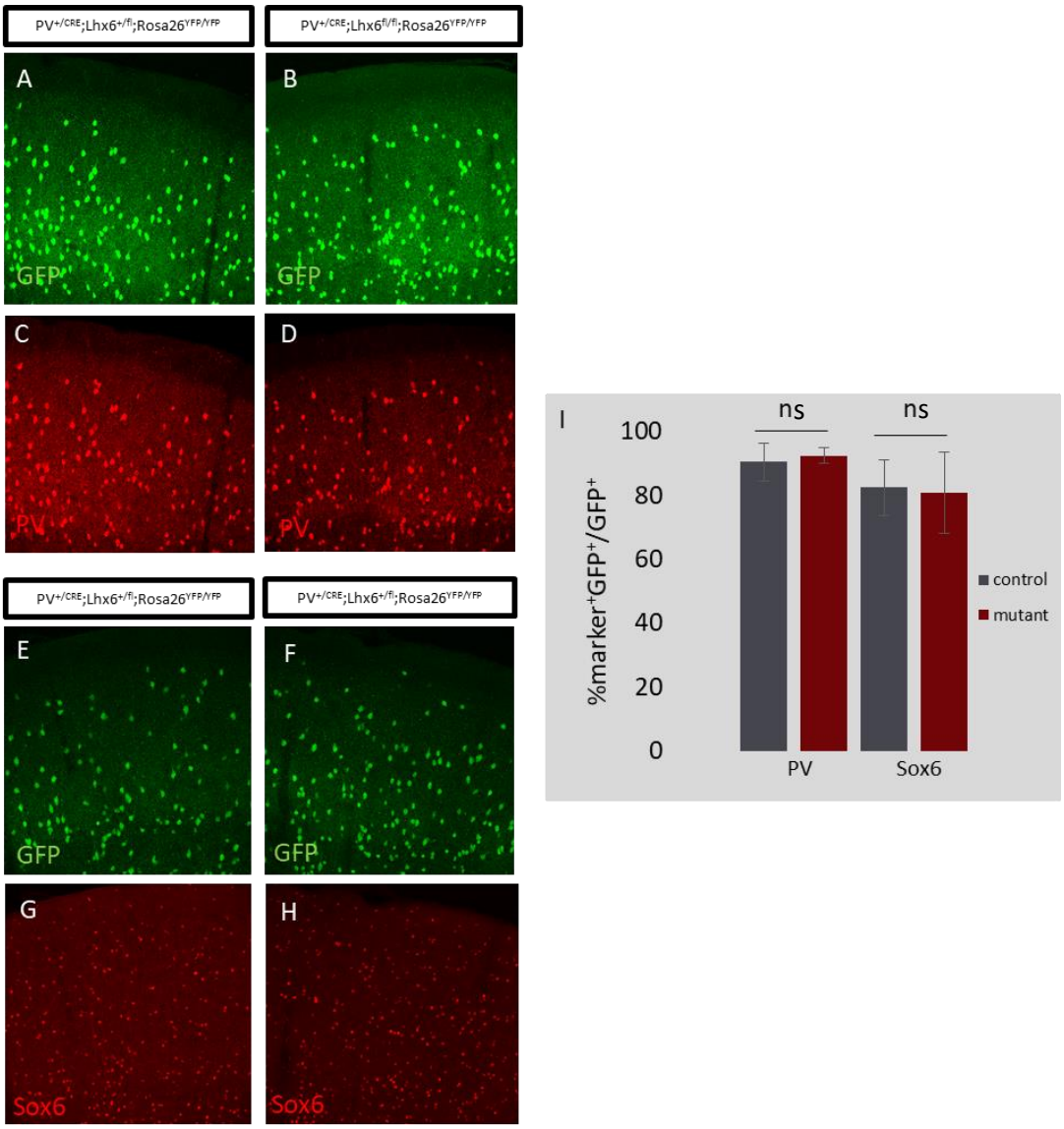

Figure S3. Aberrant molecular properties in PV-expressing cINs in the absence of Lhx6 function. (A-D, E-H) Cryosections from the somatosensory cortex of P30 control PV$^{+/CRE}$;Lhx6$^{+/fl}$;Rosa26$^{YFP/YFP}$ **(A, C, E, G)** and mutant PV$^{+/CRE}$;Lhx6$^{fl/fl}$;Rosa26$^{YFP/YFP}$ **(B, D, F, H)** littermates were immunostained with polyclonal antibody against GFP **(A, B, E, F)** PV **(C, D)** and Sox6 **(G, H)** . **(I)** Note no differences in the percentage of eYFP cINs co-labelled with antibodies against Pv and Sox6 in one month old *PVCre;Rosa26eYFP;Lhx6*$^{fl/fl}$ mice relative to *PVCre;Rosa26eYFP;Lhx6*$^{fl/+}$ controls. Data expressed as mean ± SEM. Student's t-test (two-tailed distribution, two-sample equal variance). n=3 animals per genotype.